ELECTRONIC SUPPLEMENTARY INFORMATION

Synergistic aqueous biphasic systems: a new paradigm for the 'one-pot' hydrometallurgical recovery of critical metals

Nicolas Schaeffer[†], Matthieu Gras[‡], Helena Passos[†], Vijetha Mogilireddy[‡], Carlos M.N Mendonça[†], Eduarda Pereira[†], Eric Chainet[‡], Isabelle Billard[‡], João A.P. Coutinho[†], Nicolas Papaiconomou[‡]*

[†] *CICECO, Aveiro Institute of Materials, Department of Chemistry, University of Aveiro, 3810-193 Aveiro, Portugal.*

[‡] *LEPMI - Universite Grenoble-Alpes, 1130 Rue de la Piscine, F-38000 Grenoble, France*

* Corresponding author: nicolas.papaiconomou@lepmi.grenoble-inp.fr

ǂ Nicolas Schaeffer and Matthieu Gras are equally contributing authors

The headings the Electronic Supplementary Information follows that of the article. Supplementary information referred to in a specific section of the main manuscript can be found in this document under the same section heading.

SUPPORTING INFORMATION CONTENT:

Number of pages: 13

Number of figures: 7

Number of Tables: 4

METHODOLOGY

Materials and Instrumentation

The aqueous biphasic systems (ABS) and acidic ABS (AcABS) studied in this work were established by various aqueous solutions of HCl (37 wt.% from Sigma-Aldrich) and NaCl (99.9 wt.% pure from BDH Chemicals) with the IL $[P_{44414}]Cl$. $[P_{44414}]Cl$ was purchased from Iolitec in 95 wt.% purity and was used as received. Hexahydrate cobalt and nickel chloride and tetrahydrate manganese chloride salts were purchased from Merck (99 wt.% pure). Ultrapure, double distilled water, passed through a reverse osmosis system and further treated with a Milli-Q plus 185 water purification apparatus, (18.2 MΩ.cm at 25 °C) was used for all experiments.

Single metal solution concentration before and after extraction was obtained using a PinAAcle 900F (Perkin Elmer) atomic absorption spectrophotometer (AAS). Metal concentration in multi-element solutions was determined by inductively coupled optical emission spectroscopy (ICP-OES) using a Jobin Yvon Activa spectrometer. $[P_{44414}]^+$ concentration was analysed by ^{1}H-NMR with benzene as internal standard (300 MHz Bruker Avance III spectrometer). Chloride and acid concentrations of the ABS-AcABS IL-rich phase after extraction were established using a Metrohm 904 Titrando with a chloride electrode and automatic 0.1 mol.L^{-1} NaOH titrator respectively. An 831 KF Coulometer (Metrohm) was used to determine the water content of the upper phases. The morphology of the obtained deposits was analysed by scanning electron microscopy (SEM) with energy-dispersive X-ray spectroscopy (EDS) using a Hitachi S4100 microscope. The crystal structure of the deposits was determined by X-ray powder diffraction using a Bruker AXS; the resulting diffractograms were analysed using the X'pert Highscore Plus software package.

Metal extraction in the $[P_{44414}]Cl$ – HCl – H_2O AcABS

The partition behaviour of 0.1 mol.L^{-1} single salt solutions of Co(II), Ni(II) and Mn(II) chloride in AcABS composed of 30 wt.% $[P_{44414}]Cl$ was studied as function of HCl concentration ranging from 10 wt.% to 30 wt.% at 323 K. Heating the studied AcABS to 323 K was shown to increase the biphasic region thereby allowing the study of a greater HCl concentration range (Mogilireddy et al., 2018; Schaeffer et al., 2018). Analysis at higher HCl concentration is prevented by the water content of HCl itself. Typically, 2 g of an initial aqueous solution containing a concentration of HCl ranging from 10 wt.% to 30 wt.% and 0.1 mol.L^{-1} $CoCl_2.6H_2O$, $NiCl_2.6H_2O$ or $MnCl_2.4H_2O$ is mixed with 30 wt.% $[P_{44414}]Cl$ and the remaining completed with water. This solution was mechanically agitated for 5 min at 298 K until the complete dissolution of the IL. The resulting mixture was left to phase separate 60 min in a thermostatic bath at 323 K. The volume of each phase of the AcABS was measured and aliquots of the upper and lower phases were collected for metal concentration analysis by AAS after appropriate

dilution. The chloride, acid and water content of the IL rich phase (top phase) was also determined after separation of the phases.

Electrodeposition of Co(II) from ABS-AcABS

Table S1. Composition of the systems studied for the electrodeposition of Co(II).

Composition (wt. %)	**AcABS**	**ABS**	**ABS-AcABS**
$[P_{44414}]Cl$	30	30	30
HCl	25	0.0	3.7
NaCl	0.0	7.6	7.6

RESULTS AND DISCUSSION

Metal extraction in the [P_{44414}]Cl – HCl – H_2O AcABS

The ability of [P_{44414}]Cl-based AcABS to separate Co(II) from the metal ions Ni(II) and Mn(II) was determined based on the extraction behaviour of single metal ion solutions as a function of HCl concentration with the results presented in Figure S1. The phase diagrams of [P_{44414}]Cl-HCl-H_2O at various temperatures were previously reported.[1] By performing the extraction at 323 K, a wider range of HCl concentrations could be studied compared to 298 K. Figure S1 indicates that Ni(II) partitions preferentially to the lower phase, whereas Co(II) is extracted towards the upper phase and Mn(II) distributes across both phases. Extraction for all tested elements increases with HCl concentration in the studied range. Ni(II) is minimally extracted: its extraction efficiency increases from less than 0.5% at 10 wt.% HCl to 10.6% at 30 wt.% HCl. The extraction of Co(II) varies from moderately efficient to close to quantitative with the HCl composition of the AcABS. At 10 wt.% HCl, a modest Co(II) extraction efficiency of 56.3% was obtained, increasing to a maximum of 93.2 for 25 wt.% HCl (~8M HCl). Further addition of HCl decreases Co(II) extraction to 85.5%. The extraction of Mn(II) is intermediate between that of Ni(II) and Co(II), increasing linearly from 10 to 20 wt.% HCl before plateauing at higher HCl concentrations resulting in a Mn(II) extraction efficiency around 40%. Results from Figure S1 suggest that the extraction efficiency of Co(II) and thus the Co/Ni and Co/Mn separation factor can be adjusted by careful manipulation of the HCl concentration.

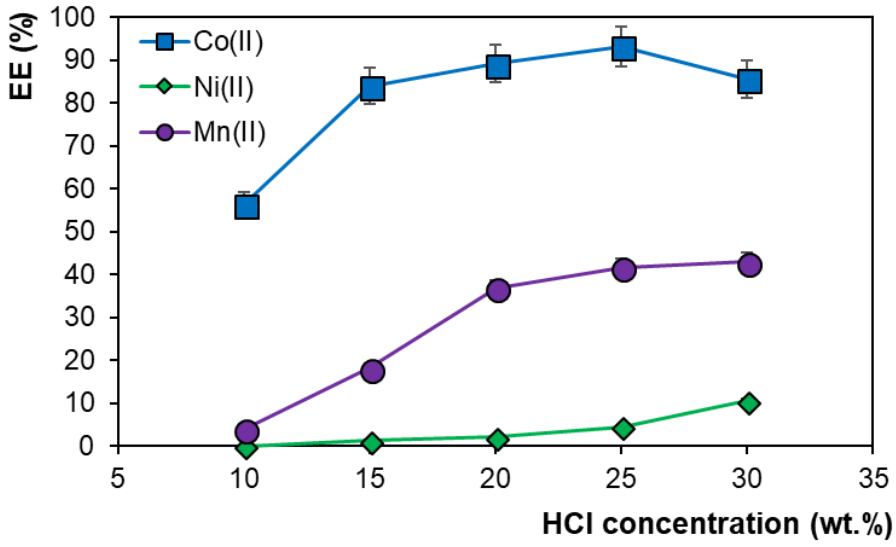

Figure S1. Extraction efficiency towards the upper phase of single ion solution of 0.1 mol.L^{-1} Co(II), Ni(II) or Mn(II) chloride in [P_{44414}]Cl-HCl-H_2O AcABS using 30 wt.% [P_{44414}]Cl as a function of HCl concentration (T= 323 K)

AcABS are tunable systems with the partitioning of the different components dependent on the temperature, acid concentration and metal loading. Knowledge of these parameters is important as they have a pronounced impact on the physical properties of the IL-rich phase, namely its transport properties (i.e. viscosity), which in turn influences the feasibility of obtaining deposits of high quality in AcABS. As such, the concentration of acid, chloride and water in the IL-rich phase after extraction were determined at the same conditions as that presented in Figure S1 and summarized in Table S2. The effect of temperature was previously studied and is not addressed here.[1] For all studied systems, the loss of the $[P_{44414}]^+$ cation to the aqueous phase is of less than 1 wt.%, further enhancing the recycling potential of this IL. An increase in the HCl content of the system results in a decrease in the water content of the IL-rich phase from 39.1 wt.% at 10 wt.% HCl to 20.3 wt.% at 30 wt.% HCl concentration. The removal of water from the IL-rich phase with increasing acid concentration results in a contraction of its phase volume. In contrast, the total acid content of the $[P_{44414}]$Cl-rich phase rises with the initial acid concentration, increasing from 1.4 mol.L^{-1} to 3.2 mol.L^{-1}. The chloride content of the IL-rich phase mirrors the acid concentration in the latter.

Table S2. Concentration of acid ($[H_3O]^+$), chloride anion and water in the IL phase and $[P_{44414}]^+$ in the aqueous phase after extraction of 0.1 mol.L^{-1} Co(II) chloride using 30 wt.% $[P_{44414}]$Cl-HCl-H_2O AcABS as a function of HCl concentration (T= 323 K) (B.D.L. – below detection limit).

System	$[H_3O]^+_{IL}$ (mol.L^{-1})	$[Cl]^-_{IL}$ (mol.L^{-1})	$[H_2O]_{IL}$ (wt.%)	$[P_{44414}]^+_{aq}$ (wt.%)
10 wt.% HCl	1.4 (±0.1)	2.5 (±0.2)	39.1 (±1.8)	0.73
15 wt.% HCl	1.9 (±0.2)	3.0 (±0.2)	31.2 (±1.7)	0.45
20 wt.% HCl	2.6 (±0.4)	3.6 (±0.4)	27.2 (±0.8)	0.16
25 wt.% HCl	3.0 (±0.3	4.1 (±0.5)	23.5 (±1.4)	B.D.L.
30 wt.% HCl	3.2 (±0.2)	4.2 (±0.6)	20.3 (±1.0)	B.D.L.

The inclusion of Co(II) complexes in the IL-rich phase further decreases its water content, limiting its workability. At the optimal AcABS conditions studied for Co(II) extraction (30 wt.% $[P_{44414}]$Cl, 25 wt.% HCl, 45 wt.% H_2O), the viscosity of the solution increases from 112 cP prior to extraction to 629 cP after at T=293 K (*cf.* Figure S2). This decrease in the IL-rich phase water content, and therefore the increase in its viscosity, is further exacerbated by the initial metal loading of the AcABS. For AcABS composed of 30 wt.% $[P_{44414}]$Cl and 25 wt.% HCl at T=298 K, a high maximum loading of approximately 10 g.L^{-1} of Co(II) was obtained followed by a sharp decrease in the extraction efficiency

at high Co(II) concentrations (*cf.* Figure S3 in the ESI). Under the studied conditions, the water content of the [P_{44414}]Cl-rich phase was of 29.0 wt.% for aqueous solutions containing ~1 g.L^{-1} of Co(II) compared to 14.8 wt.% at Co(II) feed concentrations of 12.3 g.L^{-1}. It is important to note that at high Co(II) concentration ([Co(II)] ≥ 10 g.L^{-1}), $CoCl_2.6H_2O$ can effectively salt itself out without the need for additional acid or chloride salt (illustrated in Figure S4), thereby strongly influencing the system behaviour.

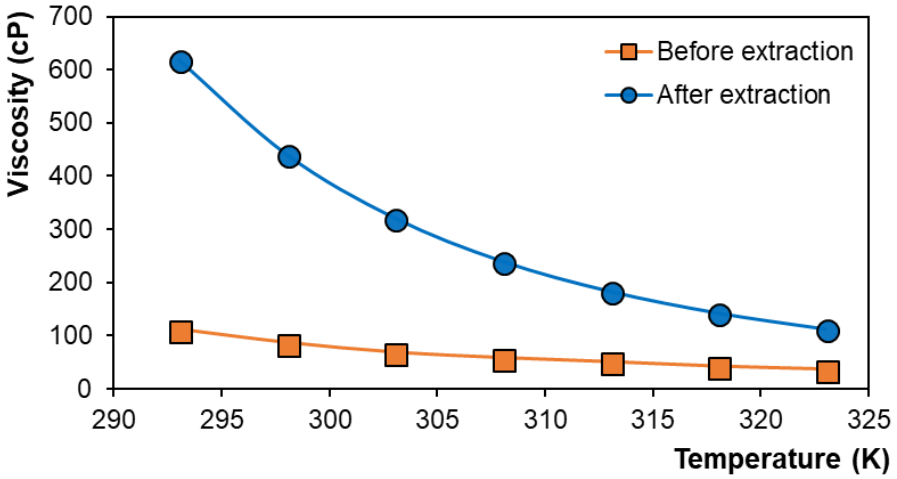

Figure S2. Viscosity of the [P_{44414}]Cl-rich phase before and after extraction of 0.1 mol.L^{-1} Co(II) (system composition: 30 wt.% [P_{44414}]Cl, 25.% HCl, 45 wt.% H_2O).

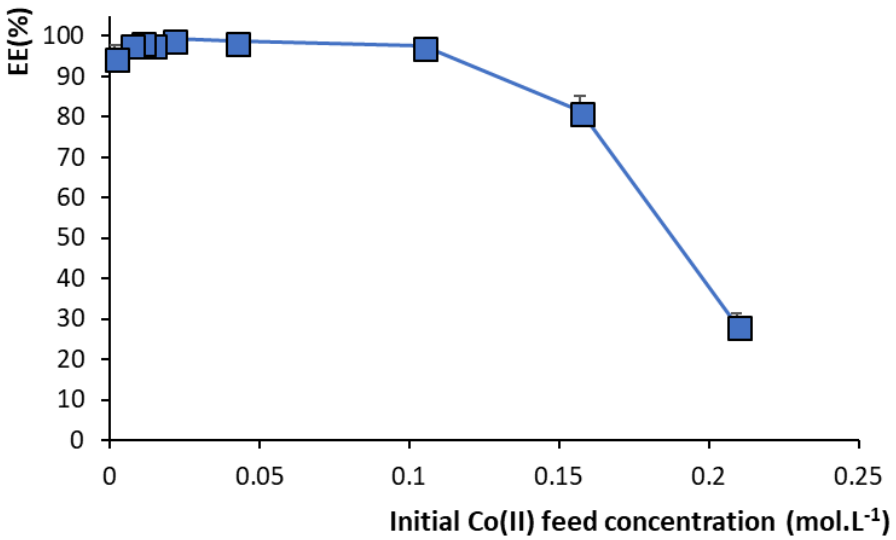

Figure S3. Extraction efficiency of 30 wt.% [P_{44414}]Cl-HCl-H_2O AcABS as a function of Co(II) concentration for a fixed 25 wt.% HCl concentration (T= 298 K).

Figure S4. Macroscopic aspect of $[P_{44414}]Cl$-$CoCl_2$-H_2O system containing 30 wt.% $[P_{44414}]Cl$ and 0.21 $mol.L^{-1}$ (12 $g.L^{-1}$) Co(II) at 323 K.

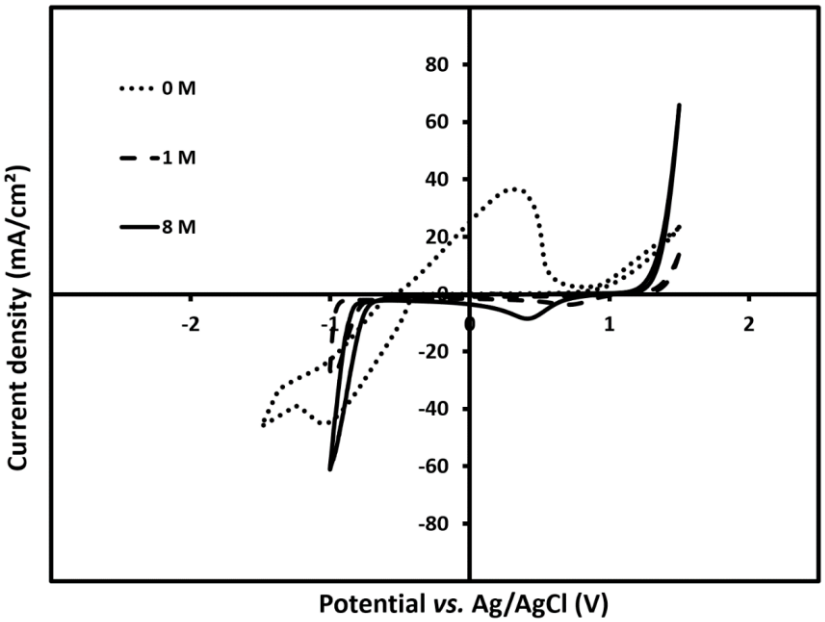

Figure S5. Cyclic voltamogram of aqueous solutions of 0.1 mol.L^{-1} of Co(II) with various concentrations of HCl (0 mol.L^{-1} to 8 mol.L^{-1}).

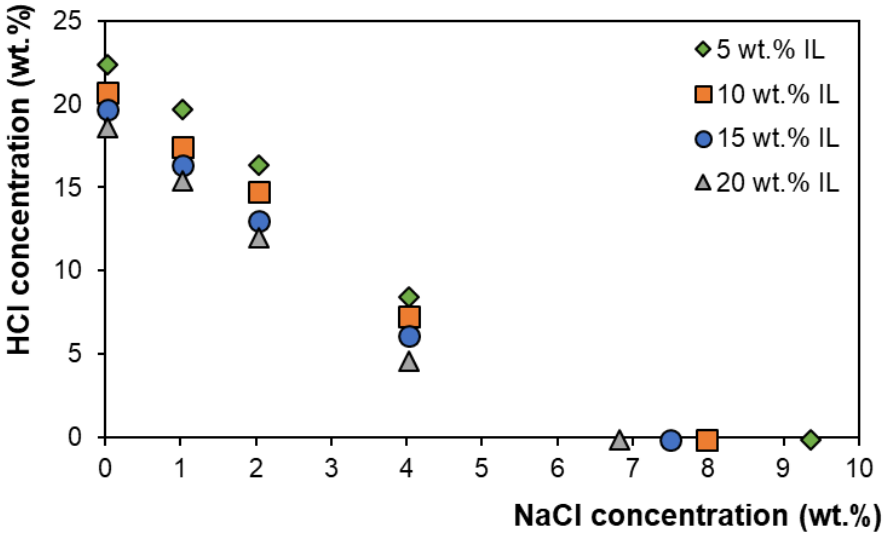

Figure S6. Reduction in the HCl concentration required to induce phase separation at a fixed NaCl concentration for 10 wt.%, 15 wt.% and 20 wt.% [P_{44414}]Cl. The data point at 0 wt.% HCl correspond to the [P_{44414}]Cl-NaCl-H_2O ABS, values taken from ref 2.

Table S3. Experimental binodal data for the HCl-[P_{44414}]Cl-H_2O-NaCl system for various NaCl concentrations at T = 298 K.

1 wt.% NaCl		**2 wt.% NaCl**		**4 wt.% NaCl**	
[P_{44414}]Cl	[HCl]	[P_{44414}]Cl	[HCl]	[P_{44414}]Cl	[HCl]
21.9	14.8	28.7	8.5	27.4	3.3
20.0	15.5	23.5	11.0	23.7	4.5
18.3	16.1	19.0	12.1	20.3	4.7
17.3	16.1	17.0	12.8	18.6	5.1
15.5	16.5	15.6	13.1	16.8	5.9
14.6	16.4	13.9	13.6	15.4	6.3
13.5	16.5	12.9	13.6	14.0	6.6
12.4	16.8	11.7	14.1	12.9	6.9
11.7	16.9	10.8	14.5	11.5	7.1
11.0	17.0	10.0	14.9	10.7	7.4
10.1	17.5	9.5	15.0	9.4	7.5
9.5	17.6	8.9	15.3	8.2	7.6
9.0	17.7	8.5	15.3	7.8	8.1
8.5	17.9	7.9	15.3	7.2	8.0
8.1	18.0	7.4	15.5	6.6	8.2
7.7	18.1	7.0	15.7	6.0	8.3
7.5	18.3	6.7	15.9	5.5	8.7
7.1	18.5	6.4	16.0	5.1	8.6
6.6	18.8	6.1	16.1	4.8	8.9
6.2	19.0	5.9	16.3	4.5	8.9
5.9	19.2	5.6	16.2	4.2	9.0
5.6	19.4	5.4	16.3	3.8	9.2
5.2	19.6	5.1	16.5	3.4	10.0
5.0	19.8	4.9	16.6	3.1	10.3
4.7	20.0	4.7	16.7	2.9	10.6
4.6	20.1	4.5	16.8	2.7	10.8
4.4	20.3	4.3	17.0	2.5	11.3

4.1	20.4	4.1	17.0	2.3	11.5
3.8	20.6	4.0	17.2	2.0	12.2
3.3	20.8	3.8	17.3	1.8	12.7
2.8	21.2	3.6	17.4	1.6	13.2
2.3	21.7	3.1	17.7	1.4	13.6
1.9	21.8	2.6	18.4	1.2	14.0
1.5	22.0	2.1	19.2	-	-
1.2	22.4	1.7	19.7	-	-

Table S4. Co(II), Mn(II) and Ni(II) extraction efficiencies (% EE) in ABS-AcABS system with varying NaCl to HCl concentrations as well as the concentration of acid (H_3O^+), chloride anion and water in the IL-rich phase after extraction at 298 K. System composition: 0.1 mol.L^{-1} of Co(II), Mn(II) and Ni(II) respectively and 30 wt.% [P_{44414}]Cl.

System composition			**% EE**			**IL-rich phase composition after extraction**		
[HCl] (wt.%)	NaCl (wt.%)	Total Cl^- (mol.L^{-1})	Co(II)	Mn(II)	Ni(II)	[H_2O] (wt.%)	H_3O^+ (mol/L)	Cl^- (mol/L)
0.0	7.6	2.7	85.6 (±1.0)	43.3 (±2.4)	4.7 (±1.0)	10.6 (±0.1)	0.015 (±0.0)	1.3 (±0.04)
3.8	5.8	3.3	89.2 (±4.6)	46.5 (±4.2)	6.9 (±1.6)	10.5 (±0.3)	0.27 (±0.02)	1.5 (±0.03)
7.2	4.9	4.2	95.5 (±3.8)	47.8 (±1.1)	6.4 (±2.4)	9.6 (±1.4)	0.32 (±0.04)	1.8 (±0.1)
10.8	4.0	5.0	97.0 (±2.2)	45.1 (±1.7)	6.3 (±1.4)	7.0 (±0.7)	0.46 (±0.06)	1.9 (±0.2)
14.5	2.8	5.9	98.6 (±2.9)	45.0 (±2.2)	6.0 (±1.3)	10.3 (±0.9)	0.57 (±0.04)	1.9 (±0.1)
18.0	1.9	6.7	99.0 (±0.5)	32.4 (±4.9)	7.2 (±3.0)	12.5 (±0.4)	1.0 (±0.1)	2.5 (±0.2)
21.7	1.1	7.6	100.7 (±8.2)	30.5 (±4.8)	6.2 (±1.7)	15.8 (±0.2)	1.6 (±0.1)	3.2 (±0.4)
24.2	0.0	8.1	98.0 (±3.3)	29.8 (±1.8)	6.4 (±1.4)	21.1 (±0.6)	2.1 (±0.1)	3.2 (±0.1)

Selective electrodeposition of Co(II) from Ni(II) and Mn(II)

The current-time transient for the deposition of Co(II) from the ABS-AcABS-diluted system was studied to determine the nucleation process. The data from the chronoamperometric experiment in Figure 7 in the manuscript was compared to the theoretical dimensionless $(i/i_m)^2$ vs. (t/t_m) curves according to the model developed by Sharifker and Hills,[3] for three-dimensional (3D) instantaneous and progressive nucleation, respectively. Comparison of the experimental and theoretical plots, presented in Figure S7, indicates that Co(0) deposition from ABS-AcABS-diluted system on a GC electrode follows the 3D instantaneous nucleation growth process. A similar observation was reported for the electrodeposition of Co(II) in the ILs $[C_4mim][BF_4]$ [4] and $[C_2mim]Cl$.[5]

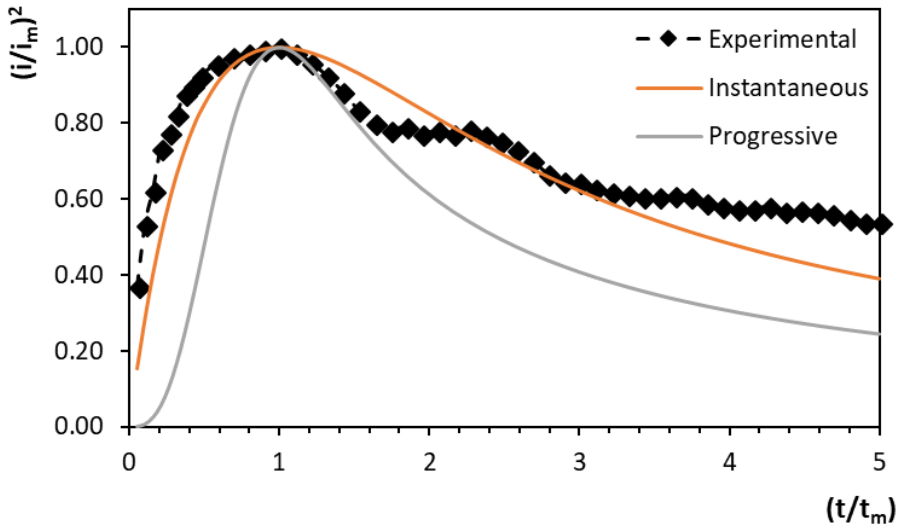

Figure S7. Comparison of the dimensionless experimental curve derived from the current–time curve for Co(II) deposition in ABS-AcABS-diluted system in Figure 7 of the manuscript with the theoretical models for 3D nucleation/growth process. Oscillation of the experimental curve is attributed to hydrogen evolution at the GC electrode.

References

1) Mogilireddy, V., Gras, M., Schaeffer, N., Passos, H., Svecova, L., Papaiconomou, N., Coutinho, J.A.P., Billard, I., Understanding the fundamentals of acid-induced ionic liquid-based aqueous biphasic system. *Phys. Chem. Chem. Phys*., **2018**, 20, 16477-16484.
2) Schaeffer, N., Passos, H., Gras, M., Mogilireddy, V., Leal, J.P., Pérez-Sánchez, G., Gomes, J.R.B., Billard, I., Papaiconomou, N., Coutinho, J.A.P., Mechanism of ionic-liquid-based acidic aqueous biphasic system formation. *Phys. Chem. Chem. Phys*., **2018**, 20, 9838-9846.
3) Scharifker, B., Hills, G., Theoretical and experimental studies of multiple nucleation. *Electrochim. Acta*, **1983**, 28, 879-889.
4) Su, C., An, M., Yang, P., Gu, H., Guo, X., Electrochemical behavior of cobalt from 1-butyl-3-methylimidazolium tetrafluoroborate ionic liquid. *Appl. Surf. Sci*., **2010**, 256, 4888-4893.
5) Hsieh, Y.T., Lai, M.C., Huang, H.L., Sun, I.W., Speciation of cobalt-chloride-based ionic liquids and electrodeposition of Co wires. *Electrochim. Acta*, **2014**, 117, 217–223.